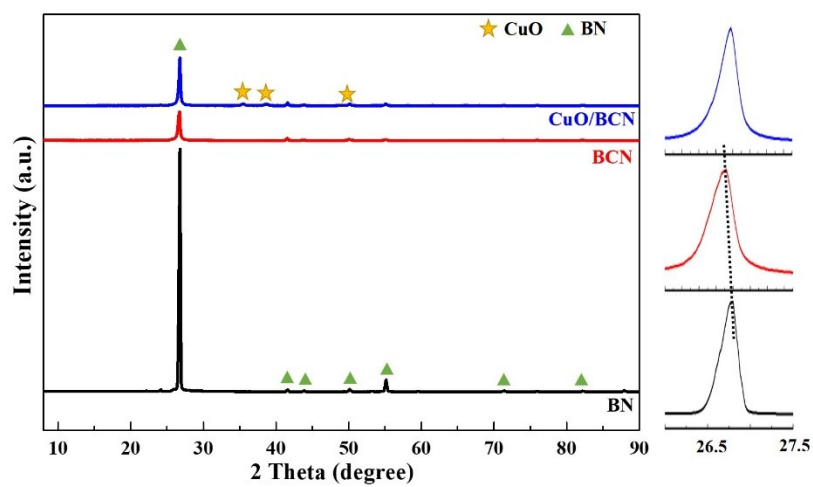**Supporting Information:**



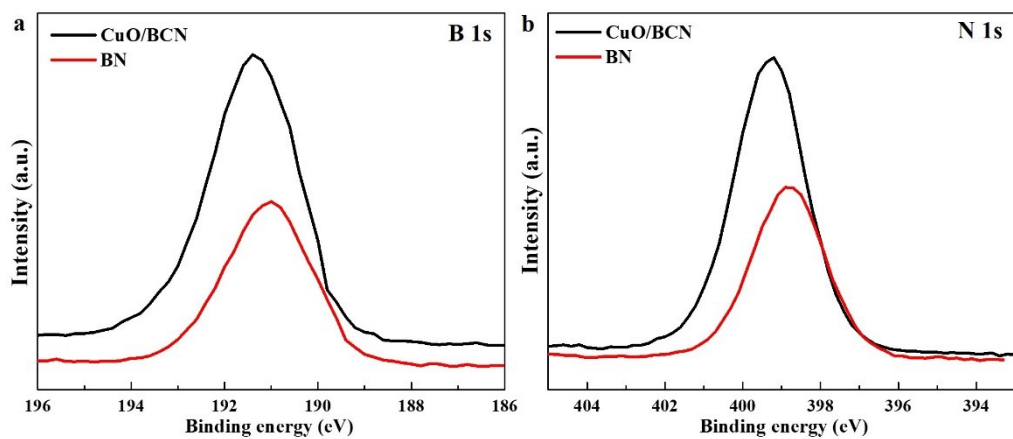Fig. S1. XRD patterns and enlarged regions of the catalysts.

Fig. S2. XPS spectra of BN and CuO/BCN catalyst: (a) B 1s and (b) N 1s.
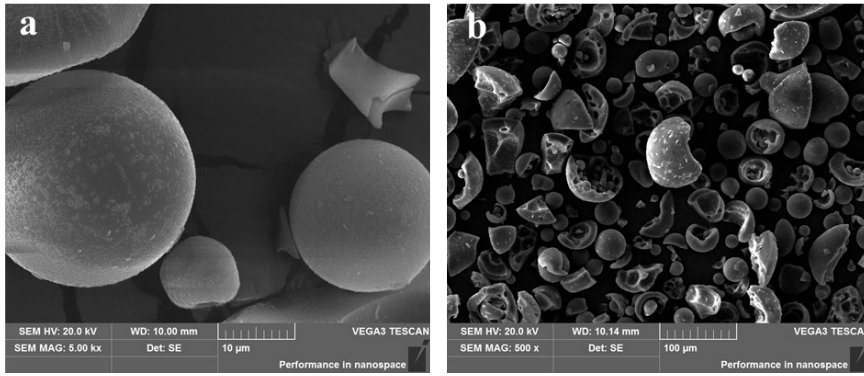
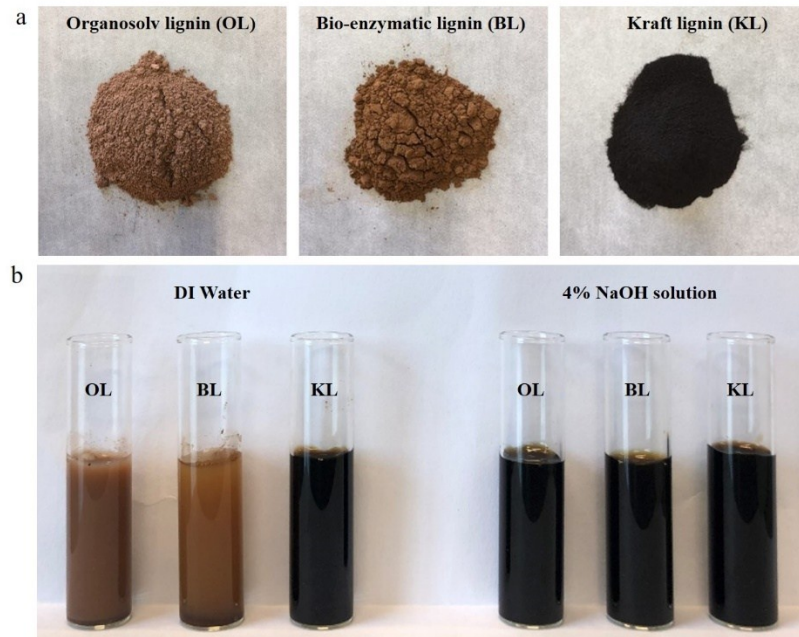Fig. S3. SEM images of KL sample (horizontal bars indicated 10 µm and 100 µm).

Fig. S4. (a) Photographs of various types of lignin with diffierent extraction methods and (b) solubility of various lignins in DI water and 4% NaOH solution (40 mg lignin, 2 mL solution).
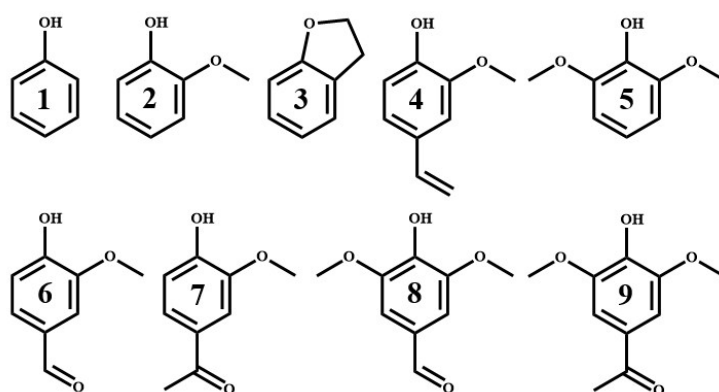
Fig. S5. Chemical structures of main aromatic monomers from depolymerization of lignin (1: Phenol; 2: Guaiacol; 3: 2,3-Dihydrobenzofuran; 4: 2-Methoxy-4-vinylphenol; 5: Syringol; 6: Vanillin; 7: Acetovanillone; 8: Syringaldehyde; 9: Acetosyringone).
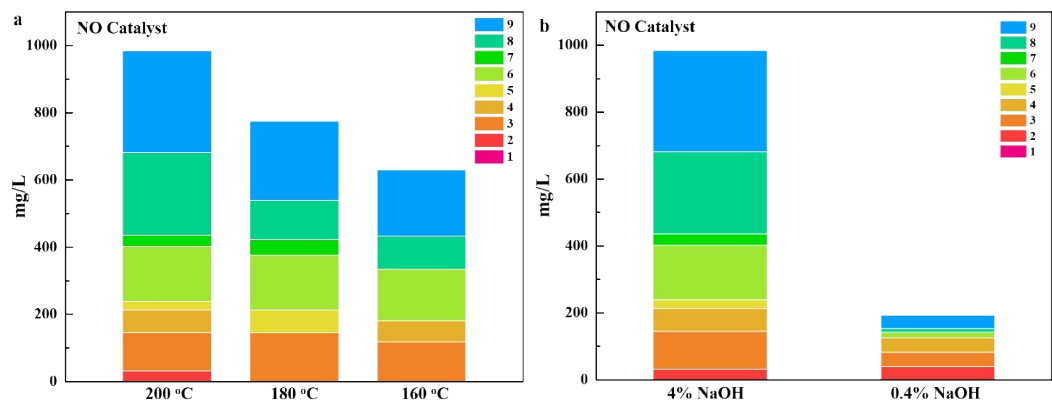
Fig. S6. (a) Temperature and (b) NaOH concentration effect on monomers yields from the depolymerization of BL (reaction conditions: 0.2 g lignin, 10 mL solution, 30 min).
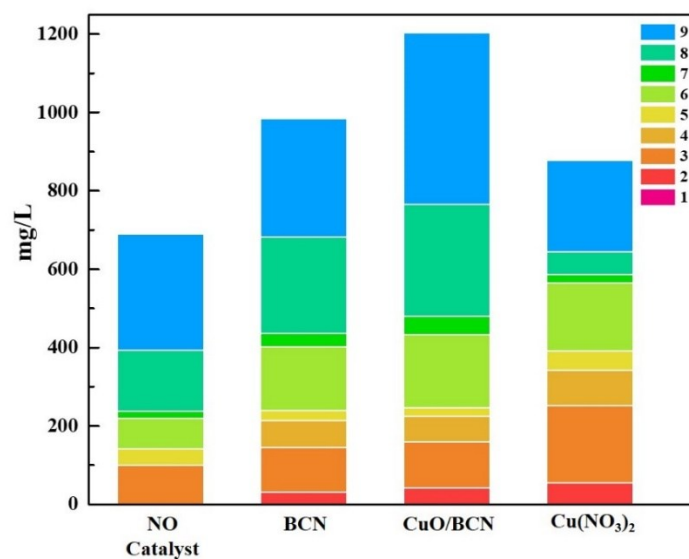
Fig. S7. Monomers yields from the depolymerization of BL over various catalysts (reaction conditions: 200 $^{\circ}$C, 0.2 g lignin, 10 mL solution, and 0.1 g CuO/BCN catalyst/30 mg Cu(NO$_3$)$_2$·3H$_2$O, 10 min).

During the reaction, the Cu(NO$_3$)$_2$·3H$_2$O could be transformed into CuO species in the alkaline solution at 200 $^{\circ}$C. The CuO loading of CuO/BCN catalyst was 10 wt%, Cu(NO$_3$)$_2$·3H$_2$O (30 mg) as the catalyst was explored for comparison.
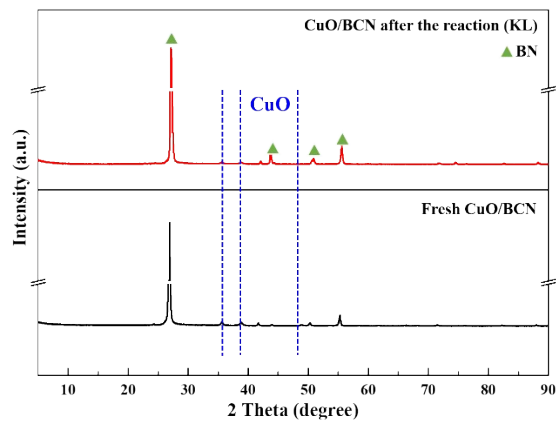
Fig. S8. XRD patterns of the catalysts after the conversion of KL.

We evaluated the spent catalyst by XRD (Fig. S8), and the experimental evidence indicated that no sulphur-containing species were detected after the depolymerization of KL. The sulphur species should be incorporated in the KL structure as the sulphur-containing functional groups would be difficult to remove at the tested temperature. Therefore, the lower yield of monomer and bio-oil from KL was mainly related to the its inert structure rather than catalyst deactivation.
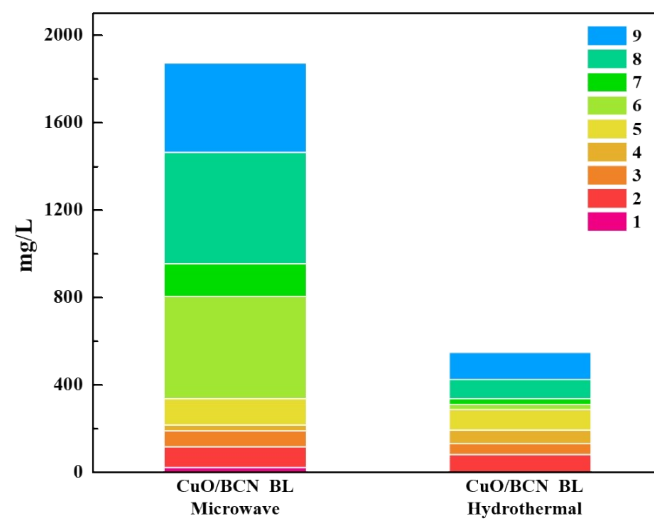
Fig. S9. Monomers yields from the depolymerization of BL by microwave and hydrothermal process (reaction condition: 0.2 g lignin, 10 mL solution, 0.1 g CuO/BCN catalyst, 30 min).
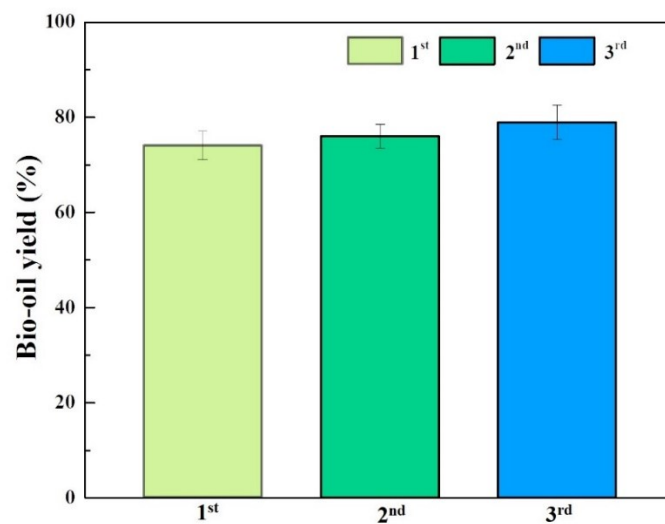
Fig. S10. Bio-oil yield from depolymerization of BL (reaction conditions: 200 $^{\circ}$C, 0.2 g lignin, 10 mL solution, 0.1 g recovered catalyst, 30 min).
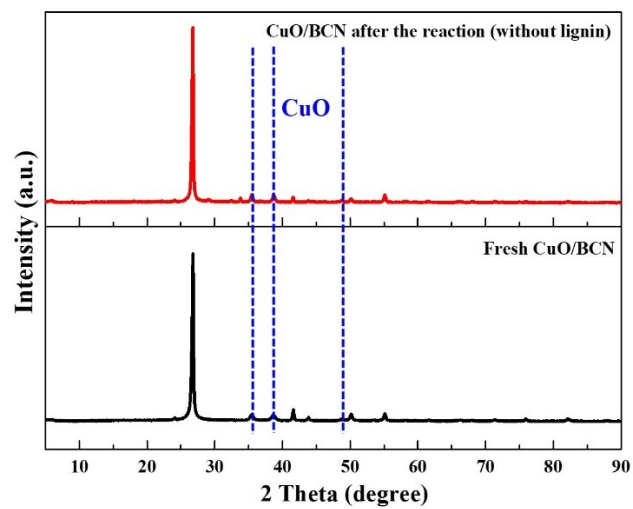
Fig. S11. XRD patterns of the catalysts.

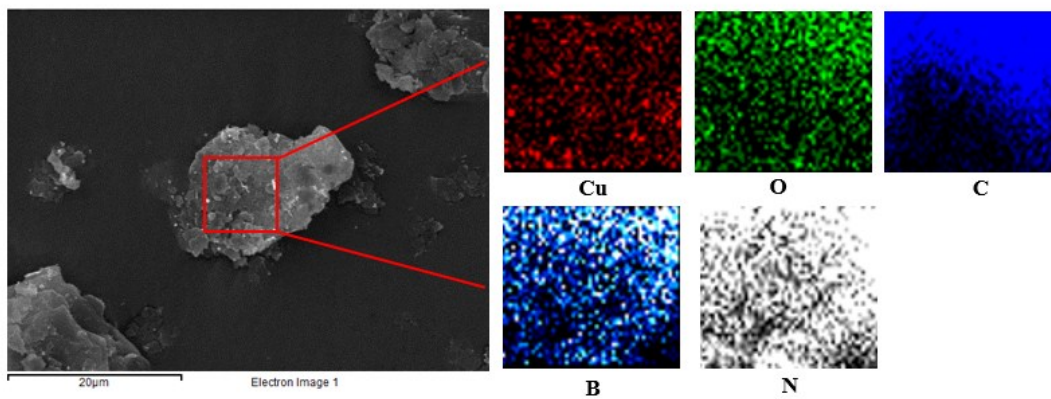Fig. S12. SEM images and elemental mapping results of CuO/BCN catalyst after three cycles.

Table S1. Physicochemical properties of various catalysts.

| Sample | BET ($m^2$/g) | Pore Volume ($cm^3$/g) | Pore Diameter (nm) |
|---|---|---|---|
| BN | 2.1 | 0.0082 | 1.5 |
| BCN | 45 | 0.19 | 2.4 |
| CuO/BCN | 39 | 0.18 | 4.0 |

Note: pore diameter was computed from the desorption branch of the isotherm using the BJH method.

Table S2. GPC analysis of various types of lignin.

| Lignin | $M_w$ (Da) | $M_n$ (Da) | Polydispersity Index |
|--------|-----------|-----------|----------------------|
| OL | 1935 | 1311 | 1.48 |
| BL | 899 | 762 | 1.18 |
| KL[a] | ~10000 | - | - |

[a] Results obtained from Sigma-Aldrich.

The harsh treatment conditions could lead to a significant decrease or even complete loss of β-O-4 structural units in KL, together with an increase of C-C linkages, which will alter the thermal stability and pyrolytic behaviour of the recovered lignin.

Table S3. Element analysis of various types of lignin (wt%).

| Lignin | N | C | H | S | O |
|--------|------|-------|------|------|-------|
| OL | 0.17 | 56.11 | 5.57 | 0 | 38.15 |
| BL | 0.85 | 56.38 | 5.68 | 0 | 37.09 |
| KL | 0.11 | 48.86 | 5.26 | 3.06 | 42.71 |